

Synthesis of nanostructured tungsten oxide by thermal oxidation method and its integration in sensor for VOCs detection

Bhagaban Behera, Sudhir Chandra*

Centre for Applied Research in Electronics, Indian Institute of Technology Delhi,
Hauz Khas, New Delhi 110016, India

*Corresponding author. Tel: (+91) 11-26591105; E-mail: sudhirchandra1950@gmail.com

Received: 18 August 2015, Revised: 24 February 2016 and Accepted: 25 May 2016

ABSTRACT

In this study, tungsten oxide nanorods have been grown by thermal oxidation of tungsten film deposited on oxidized silicon substrates for gas sensing applications. Tungsten film of thickness 100 nm was deposited by sputtering method and thermally oxidized in atmospheric ambient to synthesize nanorods. The morphology and crystal structure of tungsten oxide nanorods were characterized by scanning electron microscopy and X-ray diffraction. Also, crystal structure was verified using Raman techniques. Surface chemical composition of nanorods was analyzed using X-ray photoelectron spectroscopy. Results revealed that 100 nm film of tungsten, oxidized at 450 °C, produces nanorods of WO₃ having monoclinic structure with diameter ~100 nm and length up to 1 μm. Using standard photolithography process, Au/Cr inter digital electrodes were formed and nanorods were synthesized on it for VOCs sensing application. Sensor incorporating WO₃ nanorods exhibits very good response to ethanol, methanol and acetone vapors. The sensor response was studied at different operating temperatures for varying concentration of VOCs. The results suggest the sensor has good potential towards gas sensing applications. It is demonstrated that these sensors can detect upto 10 ppm of ethanol vapour concentration when operated at 100 °C temperature. Copyright © 2016 VBRI Press.

Keywords: Tungsten oxide nanorods; thermal oxidation; VOCs.

Introduction

There is increasing demand for gas sensors because of many applications in different sectors such as industrial productions, environmental monitoring, medical diagnosis, air quality monitoring in household etc. Metal oxide semiconductors are excellent gas sensing materials in terms of sensitivity, cost, response /recovery time and fabrication methods [1]. To date, various metal oxides including SnO, TiO, ZnO and WO have been used to detect different volatile organic compounds (VOCs) such as acetone, ethanol, methanol, 2-propanol and so on. Most of these VOCs are flammable and hazardous chemical. Exposure to such chemicals beyond certain limit is potentially dangerous to human beings. For example, acetone vapors may explode when mixed with air if the temperature exceeds beyond certain critical value. Also, VOCs detector can be used as breath analyzer. So each and every VOCs need to be detected and monitored according to its use. Nanostructured metal oxides are widely investigated due to their enhancement in functionalities and possible applications. These enhancements are possible due to increase in surface area to volume ratio as compared to bulk materials. Nanostructured tungsten trioxide (WO₃) is known to be one of the strong candidates for gas sensing application due to its fast response with high sensitivity, low humidity interferences and high thermal stability [6-7].

In the past decade, synthesis on nanostructured tungsten oxides have been extensively studied due to technological applications in gas sensors, solar cells, field emitters, photodetector, electrochromic windows, lithium-ion batteries and supercapacitors, photocatalysts [7-13]. Several methods such as thermal evaporation, chemical vapor deposition and wet chemical methods have been explored for synthesis of WO₃ nanostructures [6, 13, 14]. Thermal oxidation technique is one of the promising methods for synthesis of nanostructures metal oxide due to its simplicity, cost effectiveness, ease of large scale synthesis and high yield. Though this method has been successfully used for synthesis of ZnO and CuO nanostructures, not much information is available for tungsten oxide [15, 16]. G. Gu and C. Chen *et al.* have worked on synthesis of tungsten nanostructure by thermal annealing techniques [17, 18]. In their technique, the annealing temperature is ~750 °C and ambient is nitrogen. However thermal oxidation at relatively low temperatures in atmospheric ambient is always advantageous and it has not been explored much in the published literature. With this motivation, synthesis of WO₃ nanostructures by thermal oxidation of tungsten film has been investigated in the present work. For this purpose, WO₃ nanostructures are synthesized by thermal oxidation technique in atmospheric environment from sputter deposited tungsten film. The phase and morphology are examined by XRD (X-ray

diffraction) and SEM (scanning electron microscope) techniques. Vibration modes of nanostructures were studied using Raman spectroscopy. The influence of oxidation temperature on growth of nanorods shape and density was investigated. A sensing device was fabricated incorporating WO_3 nanostructures and the performance towards different VOCs (ethanol, acetone and methanol) has been evaluated. The sensitivity at different operating temperatures was studied to evaluate the performance of the sensor for practical applications.

Experimental

N-type Si (100) wafer having 5–10 Ω cm resistivity was selected as the starting substrate. The wafers were cleaned using 2-propanol and piranha solutions. One μm thick SiO_2 was grown on it by wet thermal oxidation technique at 1100 $^\circ\text{C}$. These substrates were mounted in RF sputtering system and 4×10^{-6} torr vacuum was created in the chamber. During deposition process, 20×10^{-3} torr argon pressure was maintained inside the chamber. Tungsten film of about 100 nm thickness was deposited from a 3" diameter tungsten target (99.99% pure) at 200 W RF power. The deposited film was then oxidized in a tube furnace at 450 $^\circ\text{C}$ for 4 h in atmospheric ambient. Morphology of post-oxidized sample was observed by SEM (Model: Zeiss, EVO 18). Crystallographic properties of nanostructures were examined using XRD (Model: X'pert). Chemical composition of the surface of nanostructures was studied using XPS (SPECS: Phoibos 100) and EDX (Model: Zeiss, EVO 50). Raman spectrum of nanostructures was studied for vibration modes using a HORIBA: LabRAM HR Evolution Raman spectroscopy. A sensor was fabricated using inter digital electrode (IDE) of 50 nm Cr/Au film which was developed successively by sputtering, photolithography and etching process. The sensor was tested for different VOCs using a test set-up mentioned by Pandya et al. [19]. The desired concentrations of VOCs were achieved by varying N_2 and air flow rates as mentioned in Eq 1 [19].

$$C(\text{ppm}) = \frac{\frac{P^* \times L}{760 - L}}{\frac{P^* \times L}{760 - L} + L + L^*} \times 10^6 \quad (1)$$

where, C represents the concentration in ppm, L represents N_2 flow rates (sccm) through the bubbler containing VOCs liquid, L^* represents air flow rate (sccm) used for dilution and P^* is vapour pressure of the VOCs (in mm of Hg) and it is dependent on bubbler temperature. The sensing performance was calibrated for different operating temperature and concentrations.

Results and discussion

Synthesis and characterization of WO_3 nanorods

The surface morphology of the as-deposited 100 nm thick tungsten sample is shown in **Fig. 1a**. It can be observed that the surface is covered with particles having diameter ~ 100 nm. When this sample is oxidized at 350 $^\circ\text{C}$ for 4 h, nanorods are formed as shown in **Fig. 1b**. The average

diameter (**Fig. 1b**) and length of nanorods are ~ 80 and 200 nm respectively. The sample oxidized at 400 $^\circ\text{C}$ resulted in nanorods with denser distribution over the surface (**Fig. 1c**). Both length and density of nanorods were observed to increase when oxidation was performed at 450 $^\circ\text{C}$ (**Fig. 1d**). Though oxidation was performed at 500 $^\circ\text{C}$ also, but the morphology of the nanorods did not change significantly (image not shown). Thus we confirm that, 100 nm thick tungsten film oxidized at 450/500 $^\circ\text{C}$ resulted in nanorods of diameter ~ 100 nm and length $\sim 1 \mu\text{m}$.

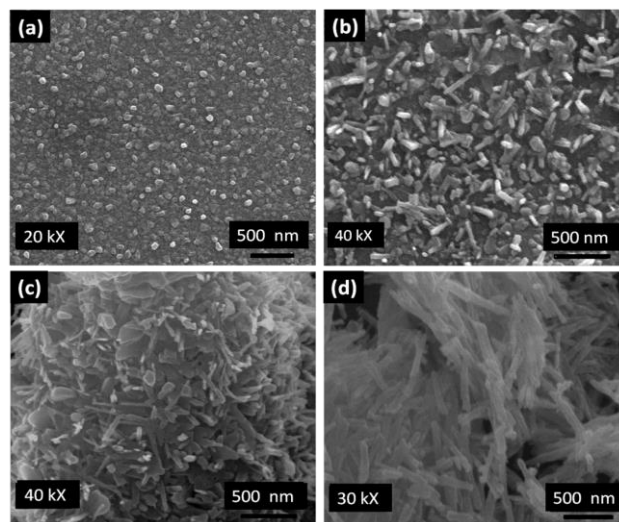


Fig. 1. SEM image of tungsten 100 nm (a) as-deposited film, (b) oxidized at 350 $^\circ\text{C}$ for 4 h, (c) oxidized at 400 $^\circ\text{C}$ for 4 h and (d) oxidized at 450 $^\circ\text{C}$ for 4 h.

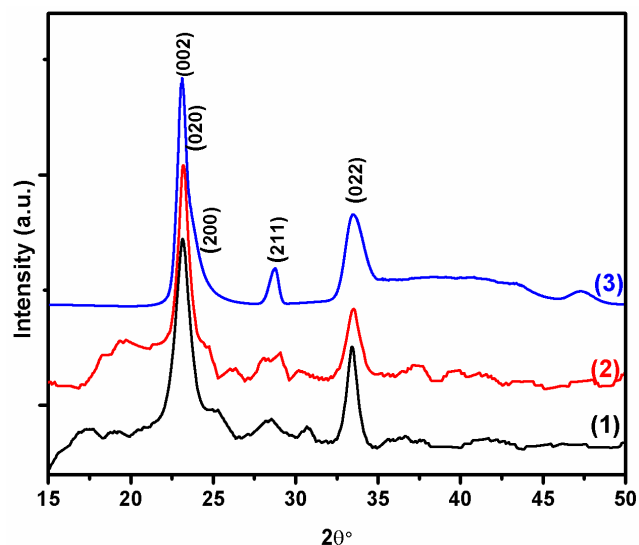


Fig. 2. XRD pattern of nanorod obtained from 100 nm tungsten films oxidized at (1) 400 $^\circ\text{C}$, (2) 450 $^\circ\text{C}$ and (3) 500 $^\circ\text{C}$

The crystal structure of the nanorods was analyzed using XRD patterns. **Fig. 2** shows the XRD pattern of nanorod synthesized from 100 nm tungsten film oxidized at (1) 400 $^\circ\text{C}$, (2) 450 $^\circ\text{C}$ and (3) 500 $^\circ\text{C}$. All these results were matched with standard JCPDS data and it was found that material is monoclinic- WO_3 having lattice parameters a

= 7.300 Å, b = 7.538 Å, c = 7.689 Å and $\beta = 90.892^\circ$. The peaks in the patterns are indexed as (002), (020), (200), (211) and (022) corresponding to 2θ values at 23.11, 23.57, 24.55, 28.87 and 33.23. Out of these five detected peaks, the intensity of (002) is relatively stronger than that of other peaks indicating that nanorods dominantly grown along the (002) direction. From highest intensity peak, the crystallite size has been calculated using Scherrer formula. The average grain size for nanorods prepared at 400, 450 and 500 °C are 21, 27 and 23 nm respectively. From the figure, it can be observed that tungsten metal is completely oxidized because no diffraction peaks corresponding to the tungsten is observed. Thus it is concluded that WO_3 nanorods with monoclinic structure can be fabricated by thermal oxidation technique at relatively low temperatures of 450 °C.

Raman spectra of nanorods prepared from 100 nm tungsten film oxidized at 400 °C and 450 °C is shown in Fig. 3. Four peaks are observed at 277, 670, 809 and 930 cm^{-1} corresponds to monoclinic phase of WO_3 . For all cases, sharp peaks are observed representing crystalline nature of materials. According to A. Baserga *et al.*, two characteristic bands of WO_3 are observed at 200-500 cm^{-1} and 600-1000 cm^{-1} [20].

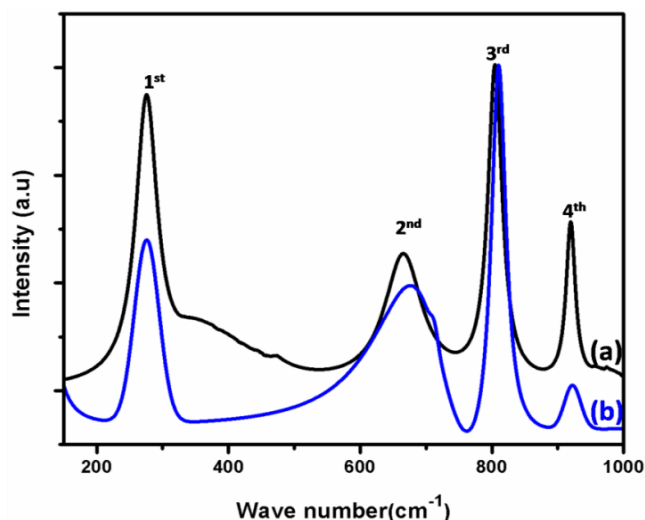


Fig. 3. Raman spectra of WO_3 nanorod obtained from 100 nm tungsten film oxidized at (a) 400 °C and (b) 450 °C.

First one is associated with O-W-O bending vibration modes whereas later one is for stretching vibration modes of W-O. The first peak at 277 cm^{-1} is very intense and sharp representing highly crystalline material. Also, third peak at 809 cm^{-1} is intense and sharp which reveals that WO_3 nanorods have stretching vibrations of bridging oxygen (O-W-O). The relative intensity of third peak for the nanorods obtained at 450 °C is higher than that of nanorods obtained at 400 °C. Thus, we can infer that nanorods synthesized at 450 °C are more crystalline in nature. Similar to third peak, the second peak centered around 670 cm^{-1} is due to stretching vibrations of the bridging oxygen atoms. The fourth peak at 930 cm^{-1} is possibly due to tungsten trioxide hydrates. Overall, all these peaks match with published work on Raman spectra of WO_3 materials [20, 21].

XPS is used to analyze chemical composition of the material surface. The XPS survey scan of nanorods was performed in the binding energy range of 0-1000 eV and corresponding spectrum is illustrated in Fig. 4a. All these obtained peaks are calibrated with respect to C1s peak (284.6 eV). Detected carbon is attributed to the environmental exposure after synthesis process. It is observed that only tungsten and oxygen are detected elements in the nanorods. The nanorods contain no other elements proving that nanorods are highly pure.

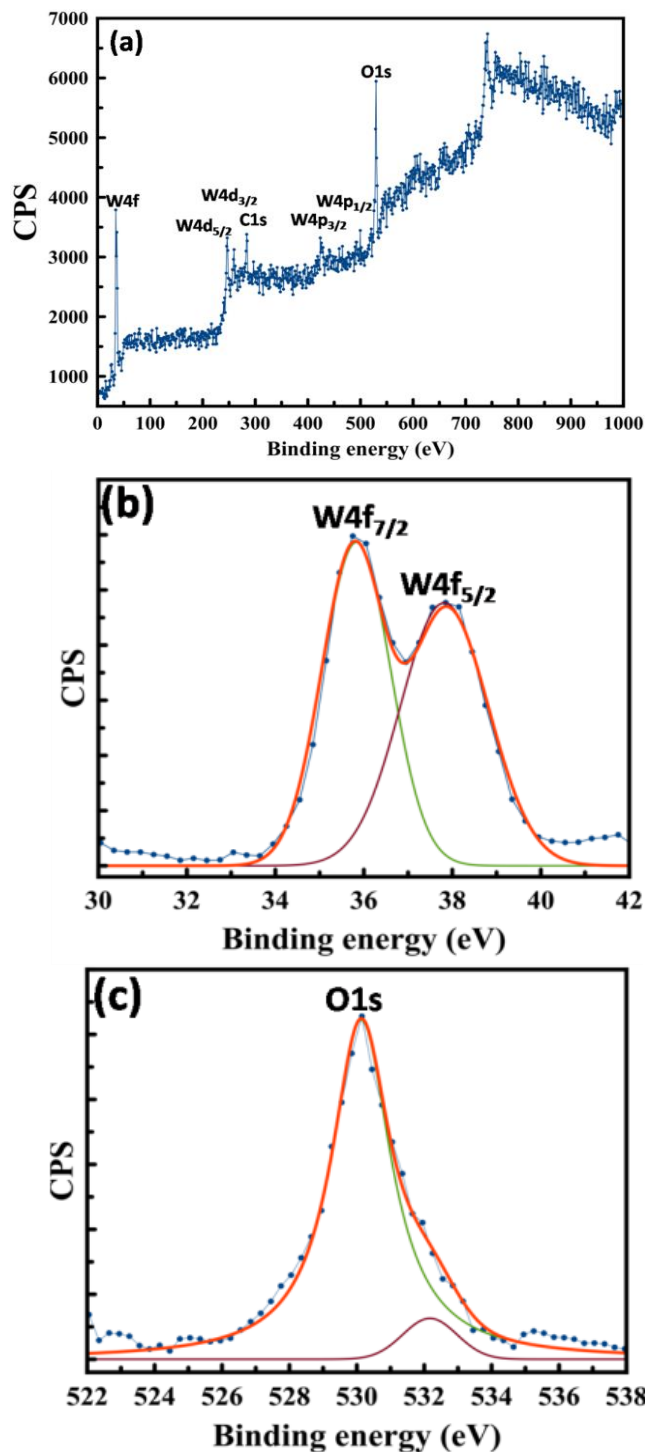


Fig. 4. (a) XPS survey scan of WO_3 nanorods (b) core level doublet spectra of W4f (c) core level spectra of O1s.

Fig. 4(b-c) show the core level doublet spectra of W 4f_{7/2} and W 4f_{5/2} at 35.8 eV and 37.9 eV and singlet O1s at 530.1 eV respectively. All these peaks were fitted using Gaussian-Lorentzian fitting as shown **Fig 4(b-c)**. The intensity ratio for W4f doublet peaks is 5:4 and binding energy separation is 2.1 eV. These results are in agreement with published results of tungsten trioxide [22]. Thus we can say that tungsten is in six-valence state (W⁶⁺). This suggests that WO₃ is formed after oxidation.

Gas sensing properties of WO₃ nanorods

The tungsten film oxidized at 450 and 500 °C resulted in nanorods. To investigate gas sensing properties, nanorods synthesized at 450 °C were tested for ethanol, methanol and acetone at 200 °C operating temperature. The change in resistance of the sensor (measured using IDE structure) upon exposure of 10 ppm VOCs is presented in **Fig. 5**. It is observed that for all cases, the resistance decreases during exposure of VOCs (reducing gases) indicating WO₃ nanorods are n-type semiconductors. The change in resistance is maximum for ethanol and minimum for acetone. At this operating temperature, the response time for ethanol, methanol and acetone is 120, 170 and 150s whereas recovery times are 140, 160 and 140s respectively. Also, dynamic response is presented in the figure. For this measurement, the testing was repeated after completion of one cycle *i.e.* VOCs were introduced into the testing chamber and ventilated out of the chamber when change in resistance reached its saturation values. It is observed that WO₃ nanorods based gas sensor produces repeatable change in resistance on exposure to VOCs and shows a constant value of baseline resistance indicating a stable device behavior.

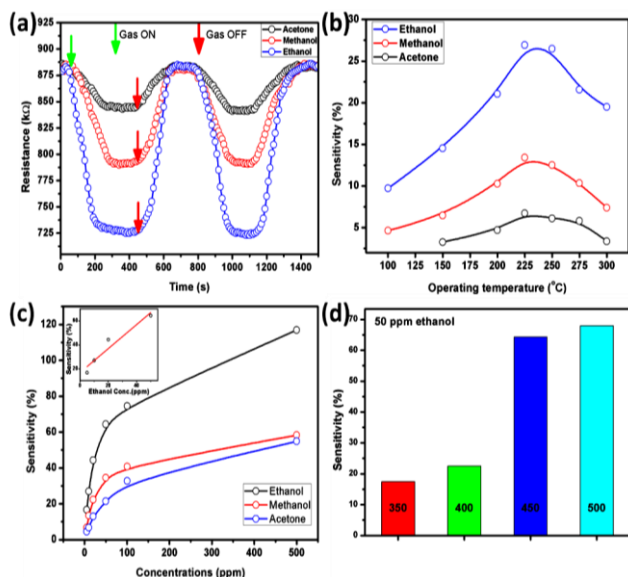
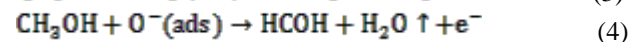
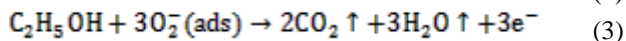
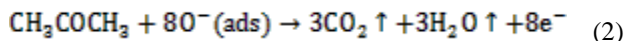


Fig. 5. (a) The sensor's change in resistance upon exposure of 10 ppm acetones, methanol and ethanol at 200 °C operating temperature (b) Sensing performance of the device for 10 ppm of VOCs over range of operating temperatures (c) Sensitivity versus VOCs concentrations of WO₃ nanorods based gas sensor at 225 °C operating temperature. The inset graph is linear plot of ethanol in 5-50 ppm range (d) Sensitivity of sensors for 50 ppm ethanol vapour concentration at 225 °C operating temperature for WO₃ nanorods prepared at 350, 400, 450 and 500 °C.

Interaction of environmental air (containing O₂) with heated WO₃, results in absorption of oxygen on the surface of sensing layer. Subsequently, electrons withdrawn from

the metal oxide leads to formation of O₂⁻, O²⁻ or O⁻ ions. This creates electron depletion layer at the surface and also at grain boundaries of nanostructures. This depletion layer creates energy barrier at the boundary of nanostructures. When sensing materials are exposed to VOCs, adsorbed oxygen ions react with VOCs as per following equations:



These emitted electrons return back to nanostructure surface to neutralize depletion layer (or lower down energy barrier). So resistance of tungsten oxide nanorods decreases during exposure of VOCs.

The results on temperature dependent sensitivity are shown in **Fig. 5(b)**. It is observed that the sensitivity is linearly increasing with temperature up to 225 °C and then decreases with further rise in temperature. The sensor shows highest sensitivity at 225 °C operating temperature and the values are 26.93, 13.4 and 6.71 for 10 ppm of ethanol, methanol and acetone respectively. Rise in sensing temperatures enhance the rate of reactions, diffusion, absorption and desorption at the surface sensing layer. At optimal working temperature, the absorption and desorption rates are balanced to give rise to maximum sensitivity. Above this temperature, desorption rate is probably more than absorption rate and hence sensitivity is lowered.

At optimal operating temperature, the sensor was tested for different concentration of VOCs. From **Fig. 5(c)**, it is observed that sensitivity is linear in the range of 5-50 ppm of VOCs and above 50 ppm, it tends to saturation. Increase in sensitivity with concentration of VOCs within 5-50 ppm can be defined by formula "S" = A×C^B, where A and B are constants which are dependent on sensing material and stoichiometry and C is the concentration of gas [23]. For higher concentrations, this formula is not followed because rate of absorption at the surface of sensing layer will be more than desorption.

From **Fig. 1**, it is observed that 100 nm films oxidized at 350, 400, 450 and 500 °C results in nanorods. From **Fig. 5a**, we have confirmed that sensitivity for ethanol is higher than for other VOCs. So sensors were fabricated incorporating nanorods obtained from different process parameters and tested for 50 ppm of ethanol at 225 °C operating temperature. The sensitivity comparison is presented in **Fig. 5d**. It can be observed that sensitivity of nanorods synthesized at 500 °C is marginally larger than nanorods synthesized at 450 °C. The sensitivity of nanorods prepared at 350 °C and 400 °C is relatively lower than nanorods prepared at higher temperature. One obvious reason for such high sensitivity is the density and length of nanorods. Also, high surface area to volume ratio of nanorods allows gas molecules to get easily adsorbed and diffuse on the surface of nanorods which enhances the total

interaction volume of sensing layer, resulting in higher sensitivity.

Conclusion

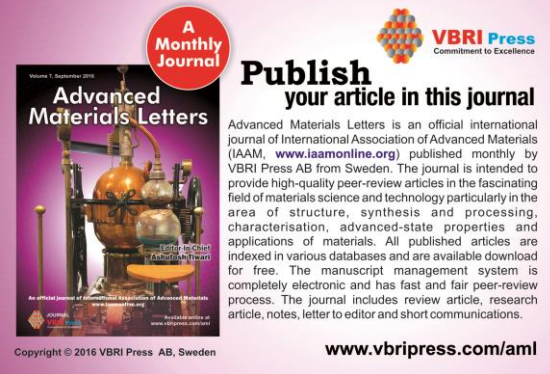
WO₃ nanorods were successfully grown on oxidized Si substrates by thermal oxidation of sputter-deposited tungsten film. The morphology and crystal structure of the WO₃ nanorods were investigated by using SEM and XRD. Oxidation temperature (450-500 °C) is one major parameter for growth of dense and long nanorods. Sensors incorporating nanorods were tested for different VOCs such as acetone, methanol and ethanol. It was found that sensor exhibits excellent sensing properties for these VOCs. In particular, WO₃ nanorods are extremely sensitive towards ethanol and can detect small concentrations (10 ppm) at relatively low temperatures (100 °C). Results showed that 225-250 °C is the optimum working temperature for detection of VOCs. The present results demonstrate that WO₃ can be synthesized by a simple technique. This is a promising technology for low-cost and high-performance sensing devices. Further studies on synthesis may be carried out so that growth mechanism can be understood. This nanostructure can be further tested for other gases such as NH₃, NO₂, H₂S to find out selective sensing performance.

Acknowledgements

Authors would like to thank National Agricultural Innovation Project (NAIP), Indian Council of Agricultural Research (ICAR) for their financial support under the project C10125 (component-4). We also very much thankful to Nanoscale Research Facility (NRF) supported from Department of Electronics and Information Technology (DeitY) India, IIT Delhi for providing assistance in characterizations.

References

- Patil, S. J.; Patil, A. V.; Dighavkar, C. G.; Thakare, K. S.; Borase, R. Y.; Nandre, S. J.; Deshpande, N. G.; Ahire, R. R; *Front. Mater. Sci.*, **2015**, *9*, 14.
DOI: [10.1007/s11706-015-0279-7](https://doi.org/10.1007/s11706-015-0279-7)
- Tan, W.; Ruan, X.; Yu, Q.; Yu, Z.; Huang, X; *Sensors*, **2014**, *15*, 352.
DOI: [10.3390/s150100352](https://doi.org/10.3390/s150100352)
- Wang, L.; Kang, Y.; Liu, X.; Zhang, S.; Huang, W.; Wang, S; *Sens. Actuators B Chem.*, **2012**, *162*, 237.
DOI: [10.1016/j.snb.2011.12.073](https://doi.org/10.1016/j.snb.2011.12.073)
- Rella, R.; Spadavecchia, J.; Manera, M. G.; Capone, S.; Taurino, A.; Martino, M.; Caricato, A. P.; Tunno, T; *Sens. Actuators B Chem.*, **2007**, *127*, 426.
DOI: [10.1016/j.snb.2007.04.048](https://doi.org/10.1016/j.snb.2007.04.048)
- Ke, M.-T.; Lee, M.-T.; Lee, C.-Y.; Fu, L.-M; *Sensors*, **2009**, *9*, 2895.
DOI: [10.3390/s90402895](https://doi.org/10.3390/s90402895)
- Ponzoni, A.; Comini, E.; Ferroni, M.; Sberveglieri, G; *Thin Solid Films*, **2005**, *490*, 81.
DOI: [10.1016/j.tsf.2005.04.031](https://doi.org/10.1016/j.tsf.2005.04.031)
- Bai, S.; Zhang, K.; Shu, X.; Chen, S.; Luo, R.; Li, D.; Chen, A; *Cryst. Eng. Comm.*, **2014**, *16*, 10210.
DOI: [10.1039/C4CE01167H](https://doi.org/10.1039/C4CE01167H)
- Rashad, M. M.; Shalan, A. E; *Appl. Phys. A.*, **2013**, *116*, 781.
DOI: [10.1007/s00339-013-8148-7](https://doi.org/10.1007/s00339-013-8148-7)
- Li, L.; Zhang, Y.; Fang, X.; Zhai, T.; Liao, M.; Sun, X.; Koide, Y.; Bando, Y.; Golberg, D; *J. Mater. Chem.*, **2011**, *21*, 6525.
DOI: [10.1039/C0JM04557H](https://doi.org/10.1039/C0JM04557H)
- Liang, L.; Zhang, J.; Zhou, Y.; Xie, J.; Zhang, X.; Guan, M.; Pan, B.; Xie, Y; *Sci. Rep.*, **2013**, *3*, 1.
DOI: [10.1038/srep01936](https://doi.org/10.1038/srep01936)
- Liu, Y.; Jiao, Y.; Zhou, H.; Yu, X.; Qu, F.; Wu, X; *Nano-Micro Lett.*, **2014**, *7*, 12.
DOI: [10.1007/s40820-014-0013-5](https://doi.org/10.1007/s40820-014-0013-5)
- Yoon, S.; Kang, E.; Kim, J. K.; Lee, C. W.; Lee, J; *Chem. Commun.*, **2010**, *47*, 1021.
DOI: [10.1039/C0CC03594G](https://doi.org/10.1039/C0CC03594G)
- Farhadian, M.; Sangpout, P.; Hosseinzadeh, G; *J. Energy Chem.*, **2015**, *24*, 171.
DOI: [10.1016/S2095-4956\(15\)60297-2](https://doi.org/10.1016/S2095-4956(15)60297-2)
- Annanouch, F. E.; Haddi, Z.; Vallejos, S.; Umek, P.; Guttmann, P.; Bittencourt, C.; Llobet, E; *ACS Appl. Mater. Interfaces*, **2015**, *7*, 6842.
DOI: [10.1021/acsami.5b00411](https://doi.org/10.1021/acsami.5b00411)
- Behera, B.; Chandra, S; *J. Nanosci. Nanotechnol.*, **2015**, *15*, 4534.
DOI: [10.1166/jnn.2015.9783](https://doi.org/10.1166/jnn.2015.9783)
- Kaur, M.; Muthe, K. P.; Despande, S. K.; Choudhury, S.; Singh, J. B.; Verma, N.; Gupta, S. K.; Yakhmi, J. V; *J. Cryst. Growth*, **2006**, *289*, 670.
DOI: [10.1016/j.jcrysgro.2005.11.111](https://doi.org/10.1016/j.jcrysgro.2005.11.111)
- Gu, G.; Zheng, B.; Han, W. Q.; Roth, S.; Liu, J; *Nano Lett.*, **2002**, *2*, 849.
DOI: [10.1021/nl025618g](https://doi.org/10.1021/nl025618g)
- Chen, C.-H.; Wang, S.-J.; Ko, R.-M.; Kuo, Y.-C.; Uang, K.-M.; Chen, T.-M.; Liou, B.-W.; Tsai, H.-Y; *Nanotechnology*, **2006**, *17*, 217.
DOI: [10.1088/0957-4484/17/1/036](https://doi.org/10.1088/0957-4484/17/1/036)
- Pandya, H. J.; Chandra, S.; Vyas, A. L; *Sens. Actuators B Chem.*, **2012**, *161*, 923.
DOI: [10.1016/j.snb.2011.11.063](https://doi.org/10.1016/j.snb.2011.11.063)
- Baserga, A.; Russo, V.; Di Fonzo, F.; Bailini, A.; Cattaneo, D.; Casari, C. S.; Li Bassi, A.; Bottani, C. E; *Thin Solid Films*, **2007**, *515*, 6465.
DOI: [10.1016/j.tsf.2006.11.067](https://doi.org/10.1016/j.tsf.2006.11.067)
- Garcia-Sanchez, R. F.; Ahmido, T.; Casimir, D.; Baliga, S.; Misra, P; *J. Phys. Chem. A.*, **2013**, *117*, 13825.
DOI: [10.1021/jp408303p](https://doi.org/10.1021/jp408303p)
- Shi, F.; Liu, J.; Dong, X.; Xu, Q.; Luo, J.; Ma, H; *J. Mater. Sci. Technol.*, **2014**, *30*, 342.
DOI: [10.1016/j.jmst.2013.08.018](https://doi.org/10.1016/j.jmst.2013.08.018)
- Leo, G.; Rella, R.; Siciliano, P.; Capone, S.; Alonso, J. C.; Pankov, V.; Ortiz, A; *Sens. Actuators B Chem.*, **1999**, *58*, 370.
DOI: [10.1016/S0925-4005\(99\)00098-2](https://doi.org/10.1016/S0925-4005(99)00098-2)



A Monthly Journal

Publish your article in this journal

Advanced Materials Letters

Advanced Materials Letters is an official international journal of International Association of Advanced Materials (IAAM, www.iaamonline.org) published monthly by VBRI Press AB from Sweden. The journal is intended to provide high-quality peer-review articles in the fascinating field of materials science and technology particularly in the area of structure, synthesis and processing, characterisation, advanced-state properties and applications of materials. All published articles are indexed in various databases and are available download for free. The manuscript management system is completely electronic and has fast and fair peer-review process. The journal includes review article, research article, notes, letter to editor and short communications.

Copyright © 2016 VBRI Press AB, Sweden

www.vbripress.com/aml